# SHARING VS. SPLITTING SPECTRUM IN OFDMA FEMTOCELL NETWORKS

*Omar Mehanna*

Dept. of Electrical and Computer Engineering, University of Minnesota

**ABSTRACT**

A network comprised of high-density femtocells coexisting with low-density macrocells, in an orthogonal frequency-division multiple access (OFDMA) setting, is considered. Two approaches are investigated: (1) *spectrum sharing* where macrocells and femtocells can access the same subchannels, and (2) *spectrum splitting* where macrocells and femtocells access separate portions of the spectrum. In both approaches, the trade-off between the utilized bandwidth and the signal-to-interference ratio (SIR), as femtocells or macrocells access more subchannels, is studied. The number of utilized subchannels that maximizes the average spectral efficiency for femtocells, subject to a minimum average spectral efficiency constraint for macrocells, is analyzed for both approaches, showing that the performance with spectrum splitting is better than spectrum sharing, for the considered model.

## 1. INTRODUCTION

Femtocell access points (FAPs) are short range, low cost, and low power base stations, installed by end-users for better indoor signal transmission and reception, coexisting with the macro-cellular network, and utilizing the same spectrum. Managing the cross-tier femto-macro interference is a fundamental challenge that limits the 'cohabitation dividend', and thus the appeal of large-scale femto deployment and integration with the cellular infrastructure. The currently dominant wireless standards (LTE and WiMAX) divide the available spectrum into orthogonal subchannels (i.e., OFDMA). This facilitates bandwidth splitting between femtocells and macrocells, possibly easing coexistence at the expense of limiting individual rates and aggressive spatial reuse. The goal of this work is to study this trade-off from the viewpoint of average spectral efficiency.

In [1], a coverage and interference analysis based on a realistic OFDMA macro/femtocell scenario is provided, assuming that FAPs are aware of the presence of neighboring macro- and femtocells, as well as their respective spectrum allocations. A different interference control method is proposed in [2], where femtocells adaptively allocate their power across the subchannels based on a load-spillage power control method. However, the overhead associated with acquiring information about neighboring cells in [1] and [2] is prohibitive in high density, random, and dynamic femtocell networks.

Instead of traditional network planning and optimization techniques, random Poisson point process (PPP) models have been recently used to model random wireless networks, and provide tractable and accurate analysis [3, 4, 5, 6]. In [4], a PPP model is used to model $K$ tiers of randomly located base stations (BSs) and develop tractable analysis for the coverage probability, where it is assumed that an arbitrary mobile user can connect to any BS if it provides the strongest signal. A similar model was considered in [5], where it is shown that it is generally preferred that each of the coexisting systems utilizes its own assigned spectrum, rather than allowing all systems to concurrently use the whole spectrum. The analysis in [4] and [5] assumed a single, indivisible channel; the additional degree of freedom associated with multiple frequency subchannels was not considered. On the other hand, the number of subbands partitioning the bandwidth that maximizes the spatial density of transmissions, with a constraint on the outage probability, was characterized in [6] for a single tier ad-hoc network. The analysis in [6] does not include the additional complexity associated with multiple coexisting networks. Another important difference between our work and [4, 5, 6] is that we consider a setting in which the transmission rate is adapted to the instantaneous SIR, and thus the average spectral efficiency is more appropriate than the transmission capacity, which is pertinent in fixed-rate scenarios, as a performance metric.

In this work, we model the locations of FAPs and macro base stations (MBSs) using PPPs in an OFDMA setting, and analyze the performance of two main approaches: (1) *spectrum sharing* where macrocells and femtocells can access the same subchannels, and (2) *spectrum splitting* where macrocells and femtocells access separate portions of the spectrum. It is clear that cross-tier interference limits the performance with spectrum sharing, whereas macrocells and femtocells sacrifice a portion of the spectrum to eliminate the cross-tier interference with spectrum splitting. In both cases, there is a trade-off in spectral efficiency between the utilized bandwidth and the signal-to-interference ratio (SIR), as femtocells or macrocells access more subchannels.We study this trade-off and characterize the number of subchannels accessed by femtocells and macrocells to maximize the average spectral efficiency for femtocells subject to a minimum average spectral efficiency constraint for macrocells, thus ensuring fair coexistence [5]. We show that the ratio between the maximized femtocell average spectral efficiency with spectrum sharing and with spectrum splitting is increasing (above one) as the ratio between the femtocell transmit-power and the macrocell transmit-power, or the femtocell density, increases. Hence, this work shows that it is generally better to assign separate portions of the spectrum to macrocells and femtocells, rather than sharing the same subchannels, for the considered model.

## 2. NETWORK MODEL

We consider a downlink scenario, where the random locations of FAPs are modeled as a realization of a homogeneous PPP of intensity $\lambda_F$ on the 2-D plane. MBS locations are also modeled as a realization of a PPP with a smaller intensity $\lambda_M$ [4]. We assume a *closed access* system, where at each time instance, each FAP communicates with a single femto mobile station (FMS) that is at distance $d_F$ meters away, and each MBS communicates with a single macro mobile station (MMS) that is at distance $d_M$ meters away. The fixed distance assumption can be easily relaxed to account for any random distance distribution [5]. A similar model can be used for the uplink scenario; the downlink case is considered for clarity of exposition.

A total bandwidth of $W$ Hz is divided into $L$ equal orthogonal subchannels of $W/L$ Hz each, as in OFDM. When the *spectrum sharing* approach is adopted, macrocells and femtocells have access to the same subchannels. In this case, each MBS randomly selects $K_M \in \{1, \ldots, L\}$ subchannels for transmission, while each FAP randomly selects $K_F \in \{1, \ldots, L\}$ subchannels for transmis-

Supported in part by NSF CCF grant 0747332.

sion. The received signal at any FMS or MMS, at any subchannel, suffers from interference from all (non-intended) FAPs and MBSs transmitting on the same subchannel. On the other hand, when the *spectrum splitting* approach is used, the spectrum is split between macrocells and femtocells such that $\nu L$ subchannels are allocated for macrocells, while $(1-\nu)L$ subchannels are allocated to femtocells, where $0 \leq \nu \leq 1$. In this case, each MBS randomly selects $K_M \in \{1,\ldots,\nu L\}$ subchannels for transmission while each FAP randomly selects $K_F \in \{1,\ldots,(1-\nu)L\}$ subchannels for transmission. The random subchannel selection approach is simple, analytically tractable, and practically appealing [6]. The coordination overhead that is necessary for a more intelligent subchannel allocation scheme is prohibitive in the dense and dynamic environment that is considered.

We assume that each FAP transmits with power $P_F/K_F$ on each selected subchannel, while each MBS transmits with power $P_M/K_M$ on each selected subchannel. By stationarity of the PPP, and since the subchannels are statistically identical, it suffices to analyze the behavior of a single typical receiving FMS and MMS [3]. We consider a propagation channel model with path-loss exponent $\alpha > 2$, and i.i.d fading across different selected subchannels. We also assume an interference - limited network, where thermal noise is negligible compared to the strong interference, which is a reasonable assumption in dense networks [5].

## 3. SPECTRUM SPLITTING

Here we consider the scenario where the spectrum is split between the femtocell and macrocell networks, eliminating cross-tier interference. At any receiving FMS, the locations of interfering FAPs form a homogeneous PPP with density $\lambda_F$ [7]. Define $N_M := \nu L/K_M$ and $N_F := (1-\nu)L/K_F$ such that $L = K_F N_F + K_M N_M$. Since the subchannels are randomly chosen (i.e., statistically identical), the density of FAPs using any single subchannel is thinned to $\tilde{\lambda}_F := \lambda_F/N_F$ [3]. Thus, the interference caused by all FAPs transmitting on a typical subchannel, incurred at a typical FMS that is using the same subchannel, is expressed as [6]:

$$I_F = \sum_{X_i \in \Pi_2(\tilde{\lambda}_F)} \frac{P_F}{K_F} h_i X_i^{-\alpha} \tag{1}$$

where $X_i$ and $h_i$ denote the distance and the fading channel power between the receiving FMS and the $i$-th interfering FAP, respectively, and $\Pi_2(\tilde{\lambda}_F)$ indicates the 2-D PPP describing the random interferer locations with density $\tilde{\lambda}_F$. The points of the 2-D PPP can be mapped to a 1-D PPP of unit intensity [8], yielding

$$I_F = (\tilde{\lambda}_F \pi)^{\alpha/2} \frac{P_F}{K_F} \sum_{T_i \in \Pi_1(1)} h_i T_i^{-\alpha/2} \tag{2}$$

where $\Pi_1(1)$ indicates a 1-D PPP of intensity 1 and $T_i$ is the distance between the FMS and the $i$-th nearest interfering node in a unit intensity 1-D PPP.

Therefore, the receive-SIR at a typical FMS and typical subchannel is expressed as

$$\gamma_F = \frac{\frac{P_F}{K_F} h_0 d_F^{-\alpha}}{I_F} = \frac{1}{Z_\alpha} \left( \frac{N_F}{d_F^2 \lambda_F} \right)^{\alpha/2} \tag{3}$$

where $h_0$ denotes the channel power from the intended FAP to the FMS, and the random variable $Z_\alpha$ is defined as

$$Z_\alpha := \frac{\pi^{\alpha/2}}{h_0} \sum_{T_i \in \Pi_1(1)} h_i T_i^{-\alpha/2}. \tag{4}$$

Similarly, the receive-SIR at a typical MMS/subchannel is given by

$$\gamma_M = \frac{1}{Z_\alpha} \left( \frac{N_M}{d_M^2 \lambda_M} \right)^{\alpha/2}. \tag{5}$$

When adaptive modulation and coding is used to adapt the rate to the Shannon bound for the instantaneous SIR, the expected spectral efficiency across the network becomes an important performance metric. Our objective here is to find the optimal number of subchannels, $K_F^*$ and $K_M^*$, and the optimal spectrum split ratio $\nu^*$, that maximize the expected spectral efficiency for femtocells subject to a minimum macrocell expected spectral efficiency $R_M^{\min}$. This objective ensures fair coexistence [5]. Since the subchannels are statistically identical, and each FAP (and MBS) utilizes a fraction $K_F/L$ (resp. $K_M/L$) of the bandwidth, the average spectral efficiencies (in bps/Hz) for femtocells and macrocells, respectively, are

$$R_F^{sp}(N_F,\nu) = \frac{(1-\nu)}{N_F} \mathbb{E}[\log_2(1+\gamma_F)], \tag{6}$$

$$R_M^{sp}(N_M,\nu) = \frac{\nu}{N_M} \mathbb{E}[\log_2(1+\gamma_M)]. \tag{7}$$

It is more convenient to use $N_F \in [1,(1-\nu)L]$ and $N_M \in [1,\nu L]$ instead of $K_F$ and $K_M$, respectively, in the analysis. It is clear that as $N_F$ increases, the bandwidth fraction $1/N_F$ utilized by each femto-user decreases on the one hand, but $\mathbb{E}[\gamma_F]$ increases on the other hand, resulting in a nontrivial bandwidth-SIR trade-off affecting $R_F^{sp}$ as $N_F$ increases. A similar tradeoff exists between $R_M^{sp}$ and $N_M$. It is also clear that $R_M^{sp}$ is linearly increasing with $\nu$, whereas $R_F^{sp}$ is linearly decreasing with $\nu$. Note that there is no dependency between the optimal $N_F^*$ that maximizes $R_F^{sp}$ and $\nu$, or between $N_M^*$ that maximizes $R_M^{sp}$ and $\nu$, as long as $N_F \in [1,(1-\nu)L]$ and $N_M \in [1,\nu L]$.

Although no closed-form solution for the maximized femtocell average spectral efficiency, $R_F^{sp*}$, subject to $R_M^{sp} \geq R_M^{\min}$, can be obtained, the following proposition gives (tight) upper and lower bounds on $R_F^{sp*}$. Define $\delta := \mathbb{E}[Z_\alpha^{-1}]$, $\eta := \frac{-\alpha/2}{\mathcal{W}(\frac{-\alpha}{2}e^{-\alpha/2})} - 1$, and $\beta := \mathbb{E}\left[\log_2\left(1+\frac{\eta}{\delta Z_\alpha}\right)\right]$, where $\mathcal{W}(x)$ is the principle branch of the Lambert $\mathcal{W}$ function that solves $\mathcal{W}(x)e^{\mathcal{W}(x)} = x$. Note that given $\alpha$ and the channel distribution, the values of $\delta$ and $\beta$ can be easily computed numerically via Monte-Carlo simulations.

**Proposition 1.** *The maximized femtocell average spectral efficiency,*

$$R_F^{sp*} := \max_{\text{s.t. } R_M^{sp}(N_M,\nu) \geq R_M^{\min}} R_F^{sp}(N_F,\nu) \tag{8}$$

*is bounded as:*

$$\frac{(1-\nu_{ub}^*)}{\tilde{N}_F}\beta \leq R_F^{sp*} \leq \frac{(1-\nu_{lb}^*)}{\tilde{N}_F}\log_2(1+\eta) \tag{9}$$

*and the optimal split ratio is bounded as $\nu_{lb}^* \leq \nu^* \leq \nu_{ub}^*$, where,*

$$\nu_{ub}^* := R_M^{\min}\frac{\tilde{N}_M}{\beta},\ \nu_{lb}^* := R_M^{\min}\frac{\tilde{N}_M}{\log_2(1+\eta)},$$

$$\tilde{N}_F := d_F^2\lambda_F\left(\frac{\eta}{\delta}\right)^{2/\alpha},\ \tilde{N}_M := d_M^2\lambda_M\left(\frac{\eta}{\delta}\right)^{2/\alpha},$$

*assuming $\tilde{N}_F \in [1,(1-\nu^*)L]$ and $\tilde{N}_M \in [1,\nu^* L]$.*

*Proof.* Using Jensen's inequality, we obtain the upper bounds:

$$R_F^{sp} \leq \frac{(1-\nu)}{N_F}\log_2(1+\mathbb{E}[\gamma_F]),\ R_M^{sp} \leq \frac{\nu}{N_M}\log_2(1+\mathbb{E}[\gamma_M])$$

To find $N_F$ that maximizes the upper bound of $R_F^{sp}$, define $\rho := \delta(d_F^2\lambda_F)^{-\alpha/2}$, then differentiate $\frac{1}{N_F}\log_2(1+\rho N_F^{\alpha/2})$ with respect to $N_F$ and equate to zero to get:

$$\frac{\alpha}{2}\rho N_F^{\alpha/2} = (\rho N_F^{\alpha/2}+1)\log_e(\rho N_F^{\alpha/2}+1)$$

Defining $\tilde{\rho} := \frac{-\alpha/2}{\rho N_F^{\alpha/2}+1}$, we get $-\frac{\alpha}{2}e^{-\alpha/2} = \tilde{\rho}e^{\tilde{\rho}}$. Using the Lambert $\mathcal{W}$ function gives $\tilde{\rho} = \mathcal{W}\left(-\frac{\alpha}{2}e^{-\alpha/2}\right)$. Then, solving for $N_F$ yields $\tilde{N}_F$ (i.e., $\tilde{N}_F$ maximizes the upper bound on $R_F^{sp}$). Similarly, $\tilde{N}_M$ that maximizes the upper bound on $R_M^{sp}$ is obtained.

Due to the independence between $\nu$ and the optimal $N_M^*$ that maximizes $R_M^{sp}$, and since $R_F^{sp}$ is monotonically decreasing with $\nu$, this means that $\max_{N_M} R_M^{sp}(N_M, \nu^*) = R_M^{\min}$. Using

$$\max_{N_M} R_M^{sp}(N_M, \nu^*) \leq \max_{N_M} \frac{\nu^*}{N_M} \log_2(1 + \mathbb{E}[\gamma_M(N_M)]), \quad (10)$$

and solving for $\nu^*$ using $\tilde{N}_M$ (which maximizes the RHS of the inequality), the lower bound $\nu_{lb}^*$ is obtained. The upper bound $\nu_{ub}^*$ can similarly be obtained from:

$$\max_{N_M} R_M^{sp}(N_M, \nu^*) \geq \frac{\nu^*}{\tilde{N}_M} \mathbb{E}[\log_2(1 + \gamma_M(\tilde{N}_M))] \quad (11)$$

and solving for $\nu^*$. Finally, the upper and lower bounds on $R_F^{sp*}$ are obtained using similar bounds as (10) and (11), respectively. □

It is clear from proposition 1 that $\nu^*$ increases linearly with $\lambda_M$ and $R_M^{\min}$, and that $R_F^{sp*}$ is inversely proportional to $\lambda_F$. Numerous simulations have shown that the lower bound in (9) is tight, and that $\tilde{N}_F$ and $\tilde{N}_M$ are very close approximations to the optimal $N_F^*$ and $N_M^*$, respectively. This implies that $K_F^*$ is inversely proportional to $\lambda_F$ and $d_F^2$ (in addition to the linear decrease with $\nu^*$), whereas $K_M^*$ depends on $R_M^{\min}$ only (linearly increases with $R_M^{\min}$). For example, if $\lambda_M$ doubles, then $\nu^*$ and $N_M^*$ also double, such that the average macrocell interference and $\mathbb{E}[\gamma_M]$ do not change, and thus achieving $R_M^{\min}$ with the same $K_M^*$. On the other hand, if $\lambda_F$ doubles, then $K_F^*$ and $R_F^{sp*}$ decrease by half, while the average femtocell interference and $\mathbb{E}[\gamma_F]$ remain unchanged. Note that if the computed $\tilde{N}_M \notin [1, \nu^* L]$, substituting with its nearest boundary value in (10) and (11) yields the modified bounds for $\nu^*$. The bounds for $R_F^{sp*}$ if $\tilde{N}_F \notin [1, (1-\nu^*)L]$ can be similarly obtained.

## 4. SPECTRUM SHARING

Here we consider the scenario where the macrocells and femtocells share the same spectrum. Redefine $N_M := L/K_M$ and $N_F := L/K_F$. It is well known that the superposition of two independent PPPs of densities $\lambda_1$ and $\lambda_2$ is equivalent to a single PPP of density $\lambda_1 + \lambda_2$ [3]. Also, it is easy to verify that the interference caused by 2-D PPP interferers of density $\lambda$ with transmission power $P$ is equivalent to the interference caused by 2-D PPP interferers of density $\lambda P^{2/\alpha}$ and unit transmission power. Thus, the interference caused by MBSs and FAPs transmitting on a typical subchannel at a typical receiver (MMS or FMS) is (temporarily ignoring fading):

$$\begin{aligned} I_F + I_M &= \sum_{X_i \in \Pi_2\left(\frac{\lambda_F}{N_F}\right)} \frac{P_F}{K_F} X_i^{-\alpha} + \sum_{Y_i \in \Pi_2\left(\frac{\lambda_M}{N_M}\right)} \frac{P_M}{K_M} Y_i^{-\alpha} \\ &= \sum_{X_i \in \Pi_2(\bar{\lambda}_F)} X_i^{-\alpha} + \sum_{Y_i \in \Pi_2(\bar{\lambda}_M)} Y_i^{-\alpha} \\ &= \sum_{X_i \in \Pi_2(\bar{\lambda}_F + \bar{\lambda}_M)} X_i^{-\alpha} = (\bar{\lambda}_F \pi + \bar{\lambda}_M \pi)^{\alpha/2} \sum_{T_i \in \Pi_1(1)} T_i^{-\alpha/2} \end{aligned}$$

where $\bar{\lambda}_F := \frac{\lambda_F}{N_F} \left(\frac{P_F}{K_F}\right)^{2/\alpha}$ and $\bar{\lambda}_M := \frac{\lambda_M}{N_M} \left(\frac{P_M}{K_M}\right)^{2/\alpha}$. Hence, the receive-SIRs at a typical FMS and a typical MMS, respectively, are (with fading):

$$\gamma_F = \frac{P_F N_F d_F^{-\alpha}}{Z_\alpha \left(\lambda_F P_F^{\frac{2}{\alpha}} N_F^{\frac{2}{\alpha}-1} + \lambda_M P_M^{\frac{2}{\alpha}} N_M^{\frac{2}{\alpha}-1}\right)^{\alpha/2}} \quad (12)$$

$$\gamma_M = \frac{P_M N_M d_M^{-\alpha}}{Z_\alpha \left(\lambda_F P_F^{\frac{2}{\alpha}} N_F^{\frac{2}{\alpha}-1} + \lambda_M P_M^{\frac{2}{\alpha}} N_M^{\frac{2}{\alpha}-1}\right)^{\alpha/2}} \quad (13)$$

where the random variable $Z_\alpha$ is defined in (4).

Similar to the previous section, we consider the following optimization objective: for a minimum macrocell average spectral efficiency constraint $R_M^{\min}$, find $K_F^*$ and $K_M^*$ that maximize the femtocell average spectral efficiency. The expected spectral efficiency expression for femtocells is $R_F^{sh}(N_M, N_F) = \frac{1}{N_F}\mathbb{E}[\log_2(1+\gamma_F)]$, and for macrocells is $R_M^{sh}(N_M, N_F) = \frac{1}{N_M}\mathbb{E}[\log_2(1+\gamma_M)]$. It is clear that $R_F^{sh}$ and $R_M^{sh}$ are increasing in $N_M$ and $N_F$, respectively, due to the decreased cross-tier interference in each case. On the other hand, as $N_F$ increases for a fixed $N_M$, the average $\mathbb{E}[\gamma_F]$ increases (due to the decreased femto-to-femto interference), but the bandwidth ratio $1/N_F$ utilized by each femto-user decreases, resulting in a nontrivial bandwidth-SIR trade-off affecting $R_F^{sh}$ as $N_F$ increases. A similar tradeoff exists between $R_M^{sh}$ and $N_M$. Here the coupling between $N_M$ and $N_F$ adds to the complexity of the problem, in contrast to the case of spectrum splitting.

To simplify the analysis, we assume that the macrocell network density is negligible compared to the femtocell density, such that the interference caused by MBSs is negligible compared to the interference caused by FAPs. In this case, $R_M^{sh}$ is decreasing in $N_M$, while $R_F^{sh}$ no longer depends on $N_M$. Thus, it is optimal to operate using the minimal $N_M$ (i.e., $N_M^* = 1$). Define $\sigma := \left(\lambda_F d_F^2 \frac{P_F d_F^{-\alpha}}{P_M d_M^{-\alpha}}\right)^{\frac{2}{\alpha-2}}$, $\mu := 2^{\frac{2}{\alpha-2}\left(R_M^{\min} + \mathbb{E}[\log_2 Z_\alpha]\right)}$, $\psi := \left(\frac{2^{R_M^{\min}}-1}{\delta}\right)^{\frac{2}{\alpha-2}}$, $\omega_u := \frac{(\eta/\delta)^{\frac{2}{\alpha}}}{\psi}$, and $\omega_l := \frac{(\eta/\delta)^{\frac{2}{\alpha}}}{\mu}$, where $\mu$, $\psi$, $\omega_l$, and $\omega_u$ can be computed via Monte-Carlo simulations given $\alpha$, $R_M^{\min}$, and the fading distribution, with no dependency on the femtocell or macrocell network parameters. The following proposition gives an upper and a lower bound on the maximized femtocell average spectral efficiency, $R_F^{sh*}$, subject to $R_M^{sh} \geq R_M^{\min}$, neglecting the interference from MBSs.

**Proposition 2.** *Assuming that the interference from MBSs is negligible ($I_M \ll I_F$), the maximized femtocell average spectral efficiency,*

$$R_F^{sh*} := \max_{\text{s.t. } R_M^{sh}(N_F) \geq R_M^{\min}} R_F^{sh}(N_F) \quad (14)$$

*is bounded as follows:*

*(a) If $\sigma \geq \omega_u + \epsilon$, then*

$$\frac{1}{N_F^{ub}} \mathbb{E}\left[\log_2\left(1 + \frac{(\mu\sigma)^{\frac{\alpha}{2}}}{Z_\alpha}\right)\right] \leq R_F^{sh*} \leq \frac{1}{N_F^{lb}} \mathbb{E}\left[\log_2\left(1 + \frac{(\psi\sigma)^{\frac{\alpha}{2}}}{Z_\alpha}\right)\right] \quad (15)$$

*and $N_F^{lb} \leq N_F^* \leq N_F^{ub}$, where*

$$N_F^{ub} := \mu \left[\frac{P_F}{P_M}(d_M^2 \lambda_F)^{\frac{\alpha}{2}}\right]^{\frac{2}{\alpha-2}}, \; N_F^{lb} := \psi \left[\frac{P_F}{P_M}(d_M^2 \lambda_F)^{\frac{\alpha}{2}}\right]^{\frac{2}{\alpha-2}}$$

*(b) If $\sigma \leq \omega_l - \epsilon$, then*

$$\frac{1}{\tilde{N}_F}\beta \leq R_F^{sh*} \leq \frac{1}{\tilde{N}_F}\log_2(1+\eta) \quad (16)$$

*where $\tilde{N}_F = d_F^2 \lambda_F \left(\frac{\eta}{\delta}\right)^{2/\alpha}$, and $\epsilon$ is a small constant.*

*Proof.* First, note that $N_M^* = 1$ with negligible interference form MBSs, and that $R_M^{sh}$ is monotonically increasing with $N_F$, whereas $R_F^{sh}$ is increasing with $N_F$ up to a maximum value, then decreasing as $N_F$ further increases. Using Jensen's inequality to upper bound $R_M^{\min} \leq R_M^{sh}(1, N_F) \leq \log_2(1+\mathbb{E}[\gamma_M])$ and solving for $N_F$ yields $N_F^{lb}$ as a lower bound on $N_F$. No closed form analytic solution can be obtained for $N_F^{(uc)}$ that maximizes $R_F^{sh}$ without the constraint $R_M^{sh} \geq R_M^{\min}$. Instead, we maximize its upper bound obtained using Jensen's inequality, which gives $\tilde{N}_F$. The derivation steps are

similar to the ones in the proof of proposition 1. Exhaustive numerical results have shown the tightness of $\tilde{N}_F$ as an approximation for $N_F^{(uc)}$, i.e., $|\tilde{N}_F - N_F^{(uc)}| < \tilde{\epsilon}$, where $\tilde{\epsilon}$ is a small constant.

So long as $N_F^{lb} \geq \tilde{N}_F + \tilde{\epsilon}$, the optimal $N_F^*$ (with the $R_M^{sh} \geq R_M^{\min}$ constraint) is guaranteed to be larger than $N_F^{lb}$. The condition $N_F^{lb} \geq \tilde{N}_F + \tilde{\epsilon}$ is equivalent to $\sigma \geq \omega_u + \epsilon$, where $\epsilon$ is a small (positive) constant that accounts for the difference between the optimum $N_F^{(uc)}$ and its approximation $\tilde{N}_F$. In this case $N_F^*$ satisfies $R_M^{sh}(N_F^*) = R_M^{\min}$ and an upper bound on $N_F^*$, $N_F^{ub}$, can be obtained from $R_M^{sh}(N_F^*) \geq \mathbb{E}\left[\log_2\left(\frac{P_M d_M^{-\alpha} N_F^{\frac{\alpha-2}{2}}}{Z_\alpha P_F \lambda_F^{\frac{\alpha}{2}}}\right)\right]$, where solving for $N_F$ yields $N_F^{ub}$. Substituting with $N_F^{lb}$ and $N_F^{ub}$ in $R_F^{sh}$ yield the bounds given in (15). On the other hand, so long as $N_F^{ub} \leq \tilde{N}_F - \tilde{\epsilon}$, the optimal $N_F^*$ is $N_F^{(uc)}$ that maximizes $R_F^{sh}$, with no constraint. This condition is equivalent to $\sigma \leq \omega_l - \epsilon$. The bounds (16) are obtained following the proof of proposition 1. □

Note that taking the interference from MBSs into consideration decreases $R_F^{sh*}$, which means that the upper bounds in (15) and (16) are also valid for the general case. According to proposition 2, we say that the network is operating in the *strong-femto-interference regime* if the network parameters satisfy $\sigma \geq \omega_u + \epsilon$, while the network is said to be operating in the *weak-femto-interference regime* if the network parameters satisfy $\sigma \leq \omega_l - \epsilon$. The proposition shows that in the strong-femto-interference regime, the optimal number of subchannels $K_F^*$ grows with the ratio $(P_M/P_F)^{\frac{2}{\alpha-2}}$, and with $(1/\lambda_F)^{\frac{\alpha}{\alpha-2}}$, whereas $K_F^*$ grows only with $1/\lambda_F$ in the weak-femto-interference regime.

Intuitively, the number of subchannels $K_F^*$ is restricted to be small by the macrocell network parameters in the strong-femto- interference regime, so that macro-users can achieve $R_M^{\min}$ (since larger $K_F^*$ imply larger $I_F$). On the other hand, in the weak-femto- interference regime, the number of subchannels $K_F^*$ optimizes the bandwidth-SIR tradeoff for the femtocell network, irrespective of the macrocell network parameters; this $K_F^*$ is sufficiently small allowing macro-users achieve $R_M^{\min}$. Note that increasing $R_M^{\min}$ decreases $\omega_u$ and $\omega_l$, implying that the network switches to the strong-femto-interference regime at a smaller $\sigma$. Numerous simulations indicated the tightness of the upper bound of (15), and that $N_F^{ub}$ is a close approximation to $N_F^*$ for $\sigma \gtrsim \omega_u$. This, in addition to the results of proposition 1, imply that $\tilde{N}_F$ and the lower bound of (16) are close approximations to $N_F^*$ and $R_F^{sh*}$, respectively, for $\sigma < \omega_u$.

## 5. SPLITTING VS. SHARING

In this section, we compare between the maximized femtocell average spectral efficiency with spectrum splitting and with spectrum sharing, when there is a constraint on the macrocell average spectral efficiency. Define the spectral efficiency ratio $\zeta := R_F^{sp*}/R_F^{sh*}$.

For negligible macrocell interference ($\lambda_M \ll \lambda_F$) and small $\sigma \leq \omega_l - \epsilon$, it is easy to see from propositions 1 and 2 that $\zeta = \tilde{\nu} \leq 1$, where $\tilde{\nu} := (1 - \nu^*)$, and that $\zeta$ is independent of $\sigma$ in that region (for fixed $d_M$). Note that $\tilde{\nu} \approx 1$ for small $\lambda_M$. This means that for the weak-femto-interference regime (i.e., small $\lambda_F$ or small $\frac{P_F d_F^{-\alpha}}{P_M d_M^{-\alpha}}$), the performance with spectrum sharing is approximately the same as (slightly better than) the performance with spectrum splitting. On the other hand, lower and upper bounds on $\zeta$ at the strong-femto-interference regime are obtained by cross-dividing the bounds on $R_F^{sp*}$ from (9) by the bounds on $R_F^{sh*}$ from (15):

$$\frac{\sigma\,\tilde{\nu}\beta/\omega_u}{\mathbb{E}\left[\log_2\left(1+\frac{(\psi\sigma)^{\frac{\alpha}{2}}}{Z_\alpha}\right)\right]} \leq \zeta \leq \frac{\sigma\,\tilde{\nu}\log_2(1+\eta)/\omega_l}{\mathbb{E}\left[\log_2\left(1+\frac{(\mu\sigma)^{\frac{\alpha}{2}}}{Z_\alpha}\right)\right]} \quad (17)$$

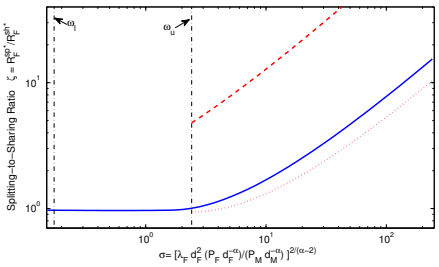


**Fig. 1**. Numerically computed $\zeta$ and its theoretical bounds vs. $\sigma$.

Next, we show that $\zeta$ *is increasing with* $\sigma$ *for sufficiently large* $\sigma$. It is easy to see that the upper and lower bounds on $\zeta$ are both increasing with $\sigma/\log_2(\sigma)$ for large $\sigma$. Since $\lim_{\sigma\to\infty} \sigma/\log_2(\sigma) = \infty$, this implies that there exists a certain threshold, $\sigma_0$, where $\zeta$ is guaranteed to be monotonically increasing with $\sigma$ for $\sigma \geq \sigma_0$. Note that the lower bound in (17) is obtained by ignoring interference from MBSs with spectrum sharing, and hence it is also valid for the general case. This shows that it is better to split the spectrum between macrocells and femtocells for large $\sigma$, where the performance advantage with spectrum splitting increases as $\sigma$ further increases.

In Fig. 1, we considered a network with $L = 1000$ subcarriers, $\lambda_M = 10^{-6}$ MBSs/m$^2$ (1 MBS per Km$^2$), $\lambda_F = 2\times10^{-3}$ FAPs/m$^2$, $d_F = 15$m, $d_M = 100$m, $R_M^{\min} = 0.5$ bps/Hz, $\alpha = 5$ (typically between 4 and 6 indoors), $P_M = 50$ dBm, and i.i.d Rayleigh fading channel. The figure shows the relation between $\zeta$ and $\sigma$, where $\sigma$ is increased by increasing $P_F$ from 0 dBm to 50 dBm. The values of $R_F^{sp*}$ and $R_F^{sh*}$ were numerically optimized to compute the ratio $\zeta$, where the expectations with respect to random locations and fading were numerically computed via more than $10^4$ Monte-Carlo simulation runs. The lower (dotted line) and upper (dashed line) bounds on $\zeta$ are also plotted for $\sigma \geq \omega_u$. The figure shows that $\zeta \approx 1$ for $\sigma < \omega_u$ (i.e., weak-femto-interference regime) whereas it is increasing with $\sigma$ for $\sigma \geq \omega_u$ (i.e., strong-femto-interference regime). The increase of $\zeta$ with $\sigma/\log_2(\sigma)$ for large $\sigma$ is also apparat in the figure. For typical $P_F = 30$ dBm ($\sigma = 15.2 > \omega_u$), the optimal $\nu^* = 0.053$, $K_F^* = 305$, and $K_M^* = 53$ yield $R_F^{sp*} = 0.58$ bps/Hz with spectrum splitting, whereas the optimal $K_F^* = 30$ and $K_M^* = 830$ yield $R_F^{sh*} = 0.25$ bps/Hz with spectrum sharing.

The relation between $\zeta$ and $\sigma$ can be intuitively explained as follows. In the weak-femto-interference regime, the decrease of $R_F^{sh*}$ due to the interference on FMSs from MBSs with spectrum sharing is approximately equivalent to the decrease of $R_F^{sp*}$ due to reserving a portion of the spectrum for macro-users. As $\sigma$ increases to the strong-femto-interference regime, the constraint $R_M^{\min}$ restricts $K_F$ to a small value to control the femto-to-macro interference, resulting in a decreased $R_F^{sh*}$, whereas there is no such restriction on $K_F$ when the spectrum is split, resulting in a relatively larger $R_F^{sp*}$.

## 6. CONCLUSIONS

We have characterized the number of utilized subchannels that maximizes the ergodic spectral efficiency for femtocells, subject to a minimum ergodic spectral efficiency constraint for macrocells, when coexisting femtocells and macrocells share, or split, the spectrum in an OFDMA setting. The provided analysis shows that it is generally better to assign separate portions of the spectrum to the macro- and femtocell networks, rather than using the same subchannels.

## 7. REFERENCES


[1] D. Lopez-Perez, A. Valcarce, G. de la Roche, and J. Zhang, *"OFDMA femtocells: a roadmap on interference avoidance," IEEE Commun. Mag.*, vol. 47, no. 9, pp. 41–48, Sept. 2009.

[2] S. Rangan, *"Femto-macro cellular interference control with subband scheduling and interference cancelation,"* submitted to *IEEE Trans. Wireless Comm.*, preprint arXiv:1007.0507, July 2010.

[3] M. Haenggi, J.G. Andrews, F. Baccelli, O. Dousse, and M. Franceschetti, *"Stochastic geometry and random graphs for the analysis and design of wireless networks," IEEE Journal on Sel. Areas in Comm.*, vol. 27, no. 7, pp. 1029–1046, 2009.

[4] H. Dhillon, R. Ganti, F. Baccelli and J. Andrews, *"Modeling and analysis of K-tier downlink heterogeneous cellular networks," IEEE Journal on Sel. Areas in Comm.*, vol. 30, no. 3, pp. 550–560, April 2012.

[5] J. Lee, J. Andrews, and D. Hong, *"Spectrum-sharing transmission capacity," IEEE Transactions on Wireless Communications*, vol. 10, no. 9, pp. 3053–3063, Sept. 2011.

[6] N. Jindal, J. Andrews and S. Weber, *"Bandwidth partitioning in decentralized wireless networks," IEEE Trans. Wireless Communications*, vol. 7, no. 12, pp. 5408–5419, Dec. 2008.

[7] D. Stoyan, W. Kendall, and J. Mecke, *Stochastic Geometry and its Applications,* John Wiley and Sons, 1996.

[8] M. Haenggi, *"On distances in uniformly random networks," IEEE Trans. on Information Theory*, vol. 51, no. 10, pp. 3584–3586, Oct. 2005.